

# Heme Oxygenase-1 Inhibits Renal Tubular Macroautophagy in Acute Kidney Injury

Subhashini Bolisetty,<sup>\*†‡§</sup> Amie M. Traylor,<sup>\*†</sup> Junghyun Kim,<sup>\*†</sup> Reny Joseph,<sup>\*†</sup> Karina Ricart,<sup>†‡</sup> Aimee Landar,<sup>†‡</sup> and Anupam Agarwal<sup>\*†‡§</sup>

<sup>\*</sup>Department of Medicine, <sup>†</sup>Division of Nephrology and Nephrology Research and Training Center, <sup>‡</sup>Center for Free Radical Biology, and <sup>§</sup>Department of Cell Biology, University of Alabama at Birmingham, Birmingham, Alabama

## ABSTRACT

Autophagy is a tightly regulated, programmed mechanism to eliminate damaged organelles and proteins from a cell to maintain homeostasis. Cisplatin, a chemotherapeutic agent, accumulates in the proximal tubules of the kidney and causes dose-dependent nephrotoxicity, which may involve autophagy. In the kidney, cisplatin induces the protective antioxidant heme oxygenase-1 (HO-1). In this study, we examined the relationship between autophagy and HO-1 during cisplatin-mediated acute kidney injury (AKI). In wild-type primary proximal tubule cells (PTC), we observed a time-dependent increase in autophagy after cisplatin. In HO-1<sup>-/-</sup> PTC, however, we observed significantly higher levels of basal autophagy, impaired progression of autophagy, and increased apoptosis after cisplatin. Restoring HO-1 expression in these cells reversed the autophagic response and inhibited apoptosis after treatment with cisplatin. *In vivo*, although both wild-type and HO-1-deficient mice exhibited autophagosomes in the proximal tubules of the kidney in response to cisplatin, HO-1-deficient mice had significantly more autophagosomes, even in saline-treated animals. In addition, ecdysone-induced overexpression of HO-1 in cells led to a delay in autophagy progression, generated significantly lower levels of reactive oxygen species, and protected against cisplatin cytotoxicity. These findings demonstrate that HO-1 inhibits autophagy, suggesting that the heme oxygenase system may contain therapeutic targets for AKI.

*J Am Soc Nephrol* 21: 1702–1712, 2010. doi: 10.1681/ASN.2010030238

Oxidative stress plays a major role in the pathogenesis of cisplatin-induced nephrotoxicity.<sup>1,2</sup> In response to injury, the kidney is able to elicit adaptive and protective mechanisms to limit further damage. One such mechanism is the rapid and robust induction of heme oxygenase-1 (HO-1).<sup>3–5</sup> Heme oxygenase is the rate-limiting enzyme in the degradation of heme to iron, carbon monoxide, and biliverdin.<sup>3,6,7</sup> Studies have shown that HO-1 mRNA is induced in the kidney as early as 3 to 6 hours in animal models of both ischemia/reperfusion and nephrotoxin-induced acute kidney injury (AKI).<sup>3,8</sup> Such induction occurs predominantly in the proximal tubule segment of the nephron,<sup>3,8</sup> which coincides with the location of maximal cisplatin accumulation and oxidative stress.<sup>9,10</sup> Chemical inhibition of HO enzyme activity in rats<sup>3</sup> and genetically deficient

HO-1 mice<sup>11</sup> treated with cisplatin have significantly worse kidney function and tubular injury, suggesting a protective role for HO-1 expression in cisplatin-induced renal tubular cell death, specifically necrosis and apoptosis.

Recent evidence indicates that autophagy, a type II programmed cell death, is induced during cisplatin injury in proximal tubular epithelial cells (PTC) and is a protective response.<sup>12–15</sup> Autophagy, a

Received March 1, 2010. Accepted May 18, 2010.

Published online ahead of print. Publication date available at [www.jasn.org](http://www.jasn.org).

**Correspondence:** Dr. Anupam Agarwal, Division of Nephrology, University of Alabama at Birmingham, 1530 3rd Avenue S., Birmingham, AL 35294. Phone: 205-996-6670; Fax: 205-996-6650; E-mail: [agarwal@uab.edu](mailto:agarwal@uab.edu)

Copyright © 2010 by the American Society of Nephrology

physiologically regulated and evolutionarily conserved process, refers to an intracellular degradation system in which cytoplasmic components, such as damaged organelles, long-lived proteins, protein aggregates, and other macromolecules, are directed to the lysosome.<sup>16–19</sup> Autophagy (also referred to as macroautophagy) begins with the formation of an initiation membrane (vesicle nucleation) that sequesters cytoplasmic components as it expands (vesicle elongation); finally, the edges fuse to form a double-membraned vesicle called autophagosome. This vesicle fuses with the lysosome to form an autolysosome where the sequestered components are degraded by the acidic lysosomal enzymes.<sup>17,20</sup> At least 31 *Atg* (*Autophagy*) genes have been identified in yeast and their mammalian orthologs have also been recently characterized.<sup>21–24</sup> Expression of the mammalian orthologs of *Atg5*, *Atg6* (beclin 1), *Atg7*, and *Atg8* (LC3, microtubule-associated protein 1 light chain 3) are used as markers to detect autophagy in mammalian cells.<sup>13,25,26</sup> Both *Atg5* and beclin play an important role in autophagosome initiation and vesicle nucleation. Vesicle elongation requires several autophagy proteins such as *Atg7* and *Atg4*. These proteins conjugate the lipid phosphatidylethanolamine to LC3 to form membrane-associated LC3-II. LC3-II is one of the autophagy proteins that specifically interacts only with the autophagic vesicles and remains associated until vesicle breakdown. All of the other proteins associate with the vesicle at different stages of maturation and have alternate functions in the cell. Therefore, LC3-II is a valuable marker to assess the presence of autophagosomes in cells.

Several *in vitro* and *in vivo* studies suggest that autophagy can induce cell survival or death depending on the stress or the cellular environment.<sup>12,13,18,22,27</sup> Under normal physiologic conditions, cells use autophagy to maintain homeostasis. If insufficient autophagy occurs, long-lived proteins and damaged organelles accumulate and cell death occurs. Even under certain pathologic conditions, autophagy is induced and is cytoprotective. However, if autophagy is prolonged or unregulated, it can lead to cell death. This suggests that autophagy may act as a cytoprotective mechanism but converges into apoptotic pathways during severe stress. Therefore, it is important to understand how autophagy is modulated as both insufficient and excessive autophagy have deleterious effects.

Because both autophagy and HO-1 are induced during cisplatin injury, the purpose of this study was to evaluate whether HO-1 expression modulated autophagy in PTC and protected them from cisplatin-induced cell death. We studied the effects of HO-1 deficiency using HO-1 knockout (HO-1<sup>-/-</sup>) mice on the progression of autophagy during cisplatin injury. Also, PTC cultures generated from HO-1<sup>+/+</sup> (heme oxygenase-1 wild-type) and HO-1<sup>-/-</sup> mice were analyzed for cisplatin-mediated autophagy and cell death. Furthermore, HO-1<sup>-/-</sup> mice that specifically express only the human HO-1 gene (HBAC mice, human HO-1 overexpressing bacterial artificial chromosome mice) were generated and PTC isolated from these mice were used to study the effects of restoring HO-1 expression on autophagy progression during cisplatin injury.

Also, ecdysone inducible HO-1 overexpressing renal epithelial cells were generated and analyzed for cisplatin-mediated autophagy.

## RESULTS

### Presence of Autophagic Vesicles in HO-1<sup>-/-</sup> and HO-1<sup>+/+</sup> Kidneys during Cisplatin Injury *In Vivo*

We have previously shown that HO-1<sup>-/-</sup> mice have worse structural (apoptosis and necrosis) and functional evidence of kidney injury after cisplatin treatment compared with HO-1<sup>+/+</sup> mice.<sup>11</sup> In this study, we examined the effects of cisplatin on autophagy in HO-1-deficient mice to evaluate if dysregulated autophagic responses contributed to increased cell death. Renal tissue examined by transmission electron microscopy (TEM) at 72 hours after saline or cisplatin administration showed that HO-1<sup>+/+</sup> and HO-1<sup>-/-</sup> mice administered cisplatin had a substantial number of autophagosomes (double-membraned vesicles with cytoplasmic content) and autolysosomes (autophagosomes that have fused with lysosomes and appear as vacuoles) in the kidney cortex, specifically in the proximal tubule segments (Figure 1). Interestingly, HO-1<sup>-/-</sup> mice that were administered saline had a higher number of autophagic vesicles (autophagosomes and autolysosomes) compared with their saline-administered HO-1<sup>+/+</sup> littermates (Figure 1).

During autophagy, soluble LC3-I is lipidated with the addition of phosphatidyl-ethanolamine to LC3-II, an insoluble form. LC3-II binds to the inner and outer membranes of the autophagosome, appearing as puncta in the cells. Renal sections from HO-1<sup>+/+</sup> mice administered saline exhibited few tubules containing punctated LC3 expression, whereas renal sections from HO-1<sup>+/+</sup> administered cisplatin exhibited a

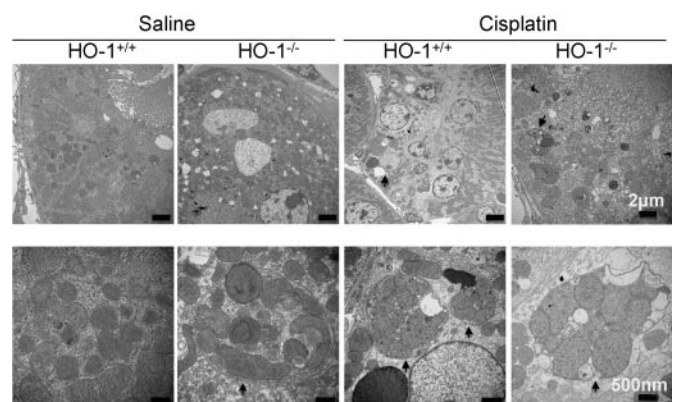


**Figure 1.** Higher number of autophagic vacuoles even in the saline-treated HO-1<sup>-/-</sup> mouse kidneys. Upper panels: Representative electron micrographs of HO-1<sup>+/+</sup> and HO-1<sup>-/-</sup> kidney cortex. Magnification,  $\times 12,000$ ; scale bar, 2  $\mu\text{m}$ . Lower panels: Representative higher magnification electron micrographs showing the presence of individual autophagic vesicles. Arrows indicate autophagosomes with double-membraned vesicles. Magnification,  $\times 30,000$ ; scale bar, 500 nm;  $n = 3$  per group.

modest increase in the number of tubules containing punctated LC3 expression, consistent with previous studies using a similar model of renal injury.<sup>13</sup> Similar to our TEM findings, HO-1<sup>-/-</sup> mice administered saline had a significantly higher level of punctated LC3-II expression compared with saline-treated HO-1<sup>+/+</sup> mice (Figure 2; Supplemental Figure 1). However, after cisplatin administration, no further increases in LC3 puncta were noted in HO-1<sup>-/-</sup> mice.

**Progression of Autophagy in PTC during Cisplatin Injury**

PTC were isolated from the HO-1<sup>+/+</sup> and HO-1<sup>-/-</sup> mice as described in the methods. The PTC were characterized by staining for  $\gamma$ -glutamyl transpeptidase (proximal tubule specific marker) and alkaline phosphatase (epithelial marker) (Supplemental Figure 2). PTC from HO-1<sup>+/+</sup> and HO-1<sup>-/-</sup> mice were treated with 50  $\mu$ M cisplatin for varying times and gene or protein expression was analyzed by real-time PCR or Western blot analysis, respectively. In the HO-1<sup>+/+</sup> PTC, expression of autophagy genes, *Atg5* and *Atg7*, was induced after cisplatin. However, HO-1<sup>-/-</sup> PTC failed to illicit a significant induction of either *Atg5* or *Atg7* after cisplatin treatment (Figure 3, A and B). Similarly, HO-1<sup>+/+</sup> PTC responded to cisplatin with an increase in *Atg5*, beclin, and LC3-II protein levels, whereas HO-1<sup>-/-</sup> PTC did not exhibit an increase above basal levels (Figure 4, A and B). Also, basal levels of LC3-II and beclin were higher in HO-1<sup>-/-</sup> PTC compared with HO-1<sup>+/+</sup> PTC (Supplemental Figure 2B). HO-1<sup>-/-</sup> PTC treated with cisplatin had significantly higher levels of cleaved caspase-3 compared with HO-1<sup>+/+</sup> PTC, indicating increased apoptosis in HO-1<sup>-/-</sup> PTC (Figure 4C).

To further characterize the role of HO-1 in regulating au-

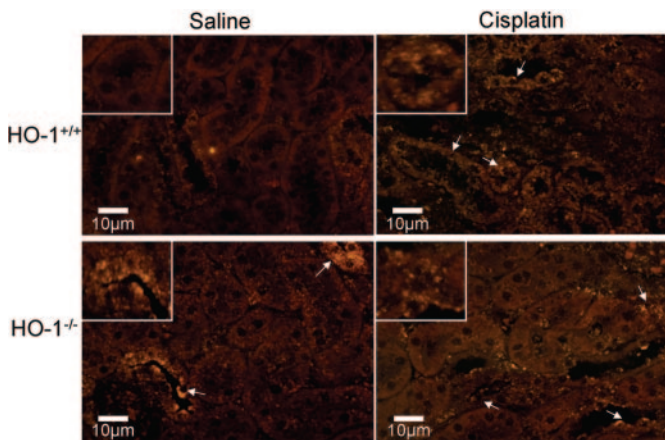


**Figure 2.** Increased punctated LC3 expression in saline-treated HO-1<sup>-/-</sup> mouse kidneys. Representative immunohistochemical staining for LC3 puncta (arrows) on paraffin-embedded kidney sections in HO-1<sup>+/+</sup> and HO-1<sup>-/-</sup> mice administered saline or cisplatin. Scale bar, 10  $\mu$ m. Inset: Higher magnification of a proximal tubule with LC3 expression showing LC3 puncta in HO-1<sup>+/+</sup> cisplatin-treated animals and HO-1<sup>-/-</sup> saline and cisplatin-treated animals; *n* = 3 to 6 per group.

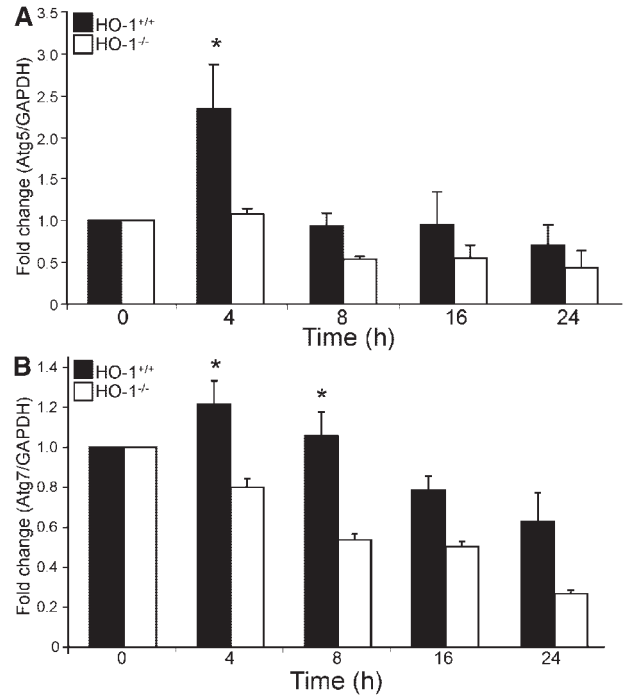


**Figure 3.** HO-1<sup>-/-</sup> primary proximal tubular epithelial cells (PTC) display blunted autophagy gene responses following cisplatin treatment. (A and B) Real-time PCR analysis of *Atg5* (A) and *Atg7* (B) expression in HO-1<sup>+/+</sup> and HO-1<sup>-/-</sup> PTC after cisplatin treatment. Results were normalized to GAPDH expression and expressed as fold change compared with their untreated controls. \**P* < 0.05 versus HO-1<sup>-/-</sup>.

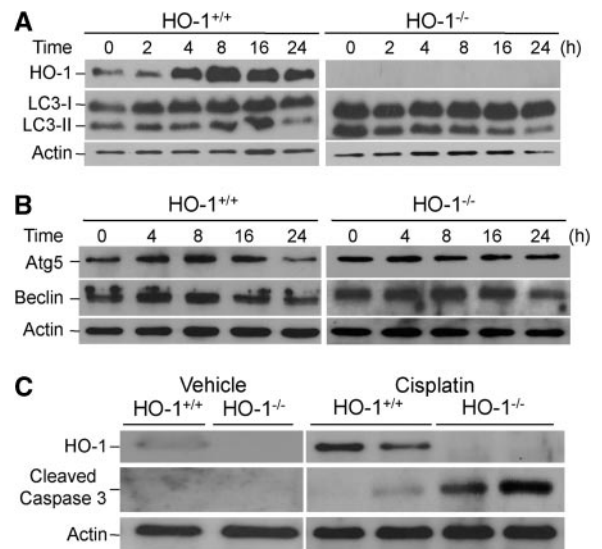


**Figure 4.** HO-1<sup>-/-</sup> PTC are unable to induce autophagy proteins following cisplatin treatment (50  $\mu$ M) compared to HO-1<sup>+/+</sup> PTC. Cell lysates were analyzed for expression of (A) LC3, (B) beclin, and (C) cleaved caspase-3 by Western blot analysis at the indicated times. The blots were stripped and probed for HO-1 and actin to confirm phenotype and loading, respectively.

tophagy, we used PTC cultured from HO-1<sup>-/-</sup> mice in which HO-1 expression was restored (HBAC mice). These mice were modified to express the human HO-1 gene so that they could be easily distinguished from the HO-1<sup>+/+</sup> mice (Kim J, Agarwal A, in preparation). As expected, HBAC PTC did not express mouse HO-1 (Supplemental Figure 3A) and, furthermore, had a significant increase (>45-fold) in human HO-1 gene expression (Supplemental Figure 3B). HBAC PTC also had an increase (>3-fold) in HO-1 protein levels compared with wild-type PTC (Supplemental Figure 3, C and D). PTC from HBAC mice responded to cisplatin in a similar manner to the HO-1<sup>+/+</sup> PTC, with induction of Atg5 and LC3-II (Figure 5A), accompanied by a decrease in cleaved caspase-3 levels (Figure 5B; Figure 6B). In addition, the high basal level of autophagy seen in the HO-1<sup>-/-</sup> PTC was attenuated. Figure 6C shows a correlative analysis of the time-dependent shift from autophagy to apoptosis in HO-1<sup>-/-</sup>, HO-1<sup>+/+</sup>, and HBAC PTC treated with cisplatin. HO-1<sup>-/-</sup> PTC show no increase in autophagy and instead exhibit higher levels of cleaved caspase-3 and undergo apoptosis more readily compared with HO-1<sup>+/+</sup> and HBAC PTC. These results suggest that expression of HO-1 is capable of rescuing the HO-1<sup>-/-</sup> PTC from impaired autophagic responses and apoptosis, further validating our finding that HO-1 is a key regulator of autophagy and apoptosis.

HO-1<sup>+/+</sup> and HO-1<sup>-/-</sup> PTC were transfected with a green fluorescence protein (GFP)-LC3 fusion plasmid and treated with 50  $\mu$ M cisplatin and examined by fluorescence microscopy for LC3 expression. Change in LC3 tagged with GFP (GFP-LC3) expression from diffuse to a punctated form is indicative of autophagosomes (Supplemental Figure 4). A time-

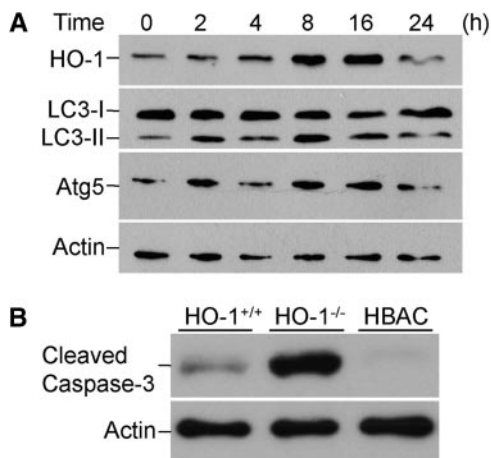


**Figure 5.** HO-1 expression restores the autophagy response and inhibits apoptosis following cisplatin treatment in PTC isolated from human HO-1 overexpressing bacterial artificial chromosome (HBAC) mice. (A) HBAC cells were treated with cisplatin (50  $\mu$ M) and cell lysates were analyzed for expression of HO-1, LC3, and Atg5. (B) HO-1<sup>+/+</sup>, HO-1<sup>-/-</sup>, and HBAC PTC were treated with 50  $\mu$ M cisplatin for 24 hours and cell lysates were analyzed for cleaved caspase-3 levels. The blots were stripped and probed for actin to confirm loading.

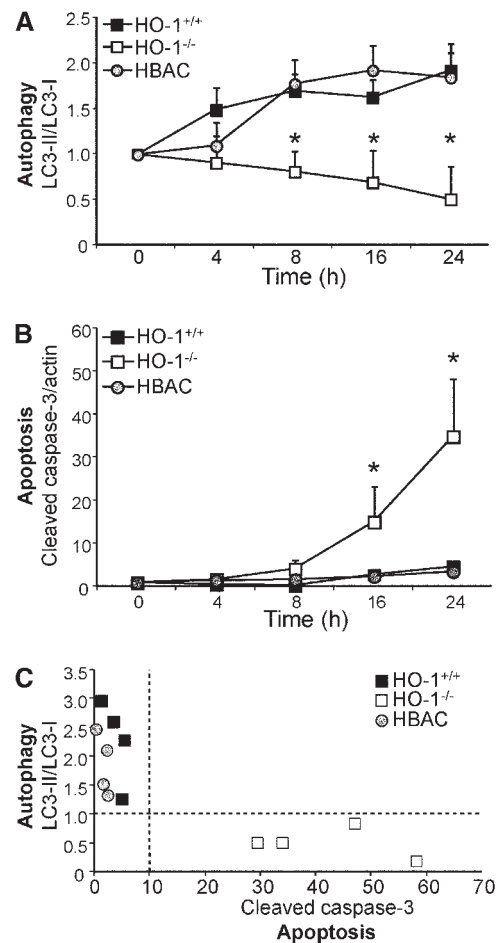


**Figure 6.** Lack of autophagy induction in HO-1<sup>-/-</sup> PTC correlates with increased apoptosis during cisplatin injury. (A) Densitometric analysis of LC3-II change (for autophagy) with cisplatin treatment. LC3-I was used as an internal loading control. \* $P < 0.05$  versus HO-1<sup>+/+</sup> and HBAC. (B) Densitometric analysis of increase in cleaved caspase-3 (for apoptosis) with cisplatin treatment. Actin was used as an internal loading control. \* $P < 0.05$  versus HO-1<sup>+/+</sup> and HBAC. (C) Correlation between autophagosome formation (LC3-II/LC3-I) and apoptosis (cleaved caspase-3/actin) after 24 hours with cisplatin. The horizontal dashed line represents the basal autophagy.

dependent increase in punctated expression of GFP-LC3 in HO-1<sup>+/+</sup> cells treated with cisplatin was observed (Supplemental Figure 4). HO-1<sup>-/-</sup> PTC had a significantly higher number of cells with punctated expression basally that did not increase further upon cisplatin treatment (Supplemental Figure 4).

### Inducible HO-1 Overexpression Protects Cells from Cisplatin-Mediated Injury

To further validate the protective role of HO-1 in cisplatin-mediated cell injury, HO-1 overexpressing (pIND/HO-1) and receptor control (RXR) cells were generated using the ecdysone inducible system. pIND/HO-1 cells responded to inducer, ponasterone A (Pon A), with an increase in HO-1

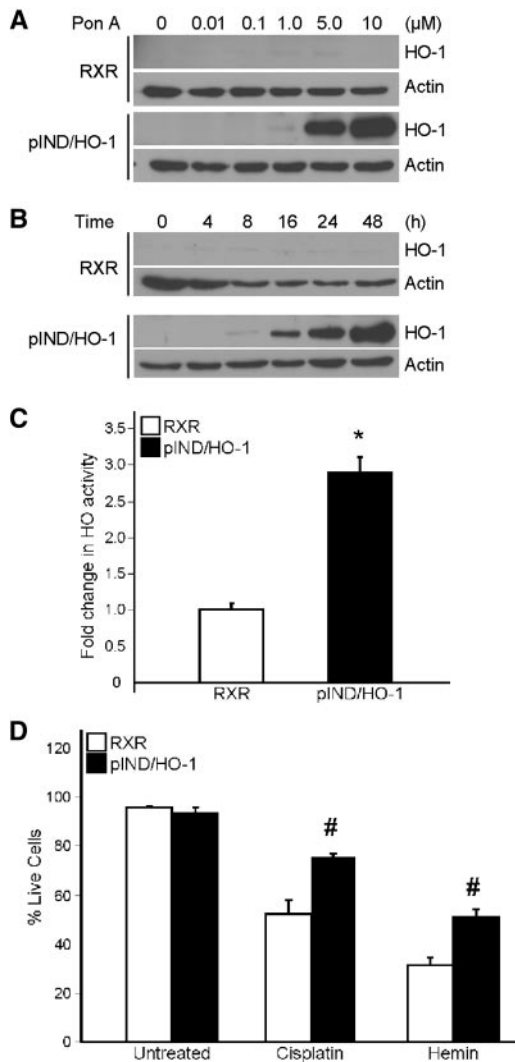


**Figure 7.** Inducible HO-1 (pIND/HO-1) overexpressing cells are protected against hemin- and cisplatin-mediated cytotoxicity. HEK293 cells were stably transfected with pIND/HO-1 (pIND/HO-1) and/or pVgRXR (RXR) plasmids and tested for HO-1 expression. (A) Western blot analysis for HO-1 in RXR and pIND/HO-1 stable cells treated with indicated doses of ponasterone A for 24 hours. (B) Western blot analysis for HO-1 in RXR and pIND/HO-1 stable cells treated with 5  $\mu$ M Pon A for various times indicated. (C) HO enzyme activity was measured in RXR and pIND/HO-1 stable cells treated with 5  $\mu$ M Pon A for 24 hours as described in Concise Methods. \* $P < 0.05$  versus RXR. (D) RXR and pIND/HO-1 stable cells were treated with 5  $\mu$ M Pon A for 24 hours, followed by treatment with cisplatin (100  $\mu$ M) or hemin (50  $\mu$ M) for 24 hours. Cell viability was determined by trypan blue exclusion assay and plotted as % live cells. # $P < 0.01$  versus RXR.

mRNA (data not shown), and protein, in a dose- and time-dependent manner (Figure 7, A and B). As expected, RXR cells did not have an increase in HO-1 protein expression above basal levels upon Pon A treatment and served as a control. Pon A-induced pIND/HO-1 cells also demonstrated a significant

increase in HO activity (>3-fold) compared with RXR cells, confirming that the overexpressed HO-1 protein was functional (Figure 7C).

RXR and pIND/HO-1 cells were induced with Pon A (5  $\mu$ M), exposed to hemin (50  $\mu$ M) or cisplatin (100  $\mu$ M) for 24 hours, and cytotoxicity was assessed by trypan blue exclusion assay. HO-1 overexpressing cells had a significant increase in cell viability compared with RXR cells that were exposed to hemin or cisplatin (Figure 7D). These results, based on the use of an inducible expression system, confirm our previous data with constitutive HO-1 overexpression demonstrating a cytoprotective role for HO-1 in cisplatin-mediated cell death.<sup>11</sup>

### Delayed Progression of Autophagy in HO-1 Overexpressing Cells

To evaluate the role of HO-1 in cisplatin-mediated autophagy, RXR and pIND/HO-1 cells were transfected with a GFP-LC3

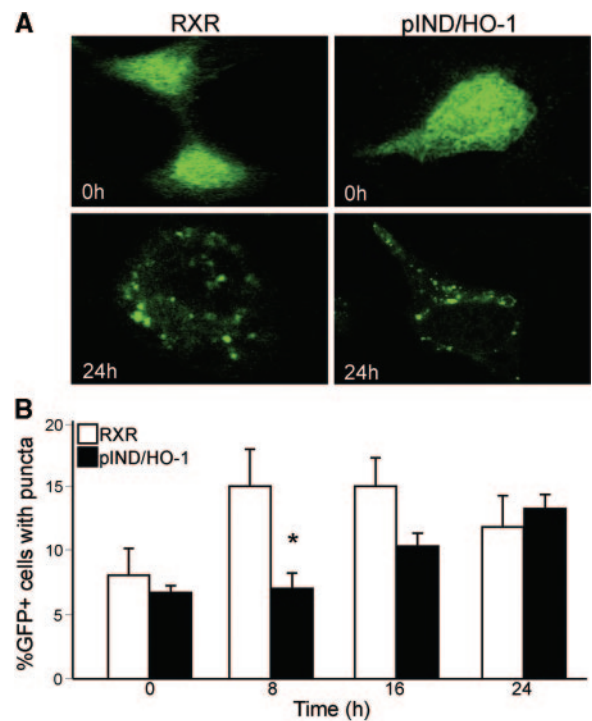


**Figure 8.** HO-1 overexpressing cells (pIND/HO-1) exhibit delayed autophagosome formation in response to cisplatin injury. RXR and pIND/HO-1 cells were transfected with GFP-LC3 plasmid and induced with 5  $\mu$ M Pon A for 24 hours, followed by treatment with 50  $\mu$ M cisplatin. At the indicated times, fluorescence images were taken, blinded, and quantitated for the presence of GFP-LC3 puncta. (A) Representative images of GFP-LC3 expression in stable cells treated with cisplatin. Formation of GFP-LC3 puncta was visible in stable cells treated with cisplatin for 24 hours compared with the diffused pattern of GFP-LC3 at 0 hours. (B) GFP-positive cells with diffuse and punctated GFP-LC3 were counted and quantitation was performed on 12 images per time point with an average of 50 cells from at least three independent experiments and expressed as % GFP cells with puncta. \* $P < 0.05$  versus RXR.

fusion plasmid, induced with Pon A and treated with 50  $\mu\text{M}$  cisplatin, and examined by fluorescence microscopy for change in LC3 expression pattern. GFP-LC3 puncta formation was evident in both RXR and pIND/HO-1 cells treated with cisplatin (Figure 8A). Quantitation demonstrated a time-dependent increase in punctated expression of GFP-LC3 in RXR cells treated with cisplatin. In contrast, pIND/HO-1 cells had a significant delay in puncta formation (autophagosome) upon cisplatin treatment compared with RXR cells (Figure 8B).

### Inhibition of Reactive Oxygen Species Generation in HO-1 Overexpressing Cells during Cisplatin Injury

Cisplatin mediates cytotoxicity through the generation of reactive oxygen species (ROS). To evaluate the role of HO-1 overexpression on ROS generation, RXR and pIND/HO-1 cells were induced with Pon A (5  $\mu\text{M}$ ) and treated with cisplatin (50  $\mu\text{M}$ ). RXR cells had an increase in ROS generation after cisplatin treatment, as evident by an increase in 2',7'-dichlorodihydrofluorescein (DCF) fluorescence (Figure 9A). However, in addition to reduced cell death (Figure 7D), pIND/HO-1 cells

had a significant inhibition of ROS generation after cisplatin treatment compared with RXR cells (Figure 9B).

## DISCUSSION

The results of this study demonstrate several important findings. First, the absence of HO-1 is associated with elevated basal autophagy (LC3-II and beclin) both *in vitro* and *in vivo*. Second, this work demonstrates for the first time that loss of HO-1 is coupled to a failure to further induce autophagy and leads to increased apoptosis after cisplatin. Third, restoring HO-1 expression in the HO-1<sup>-/-</sup> PTC reverses the increased basal levels of autophagy and impaired autophagy progression. Fourth, inducible HO-1 overexpressing cells display a delay in the onset of autophagy and have a significant inhibition of ROS generation and apoptosis during cisplatin injury. These findings underscore the importance of HO-1 expression in cisplatin-mediated autophagy.

The importance of autophagy in renal pathology is now being recognized in a wide array of injury models. Autophagosomes are detected after ischemia/reperfusion injury in mice and rats.<sup>28–31</sup> Similarly, autophagy is also induced in the kidney by a number of anticancer drugs such as tamoxifen, rapamycin, and cisplatin.<sup>13</sup> Furthermore, autophagosome-like structures are identified in transplanted kidneys in humans.<sup>28</sup> Whether the induction of autophagy in these models is protective or detrimental has been the subject of much debate. In certain *in vitro* models, inhibition of autophagy increased cell death after injury whereas in others cell death was decreased.<sup>12,13,22,28,32</sup> It is recognized however that autophagy is induced during stress, and when stress persists, it may converge into apoptotic pathways.<sup>30,31</sup> This dual nature of autophagy and the increasing number of pathologies it is associated with highlight the importance of studying the regulation and effects of autophagy during kidney injury.

Cisplatin is a chemotherapeutic agent that has been used to effectively treat solid cancers such as testicular, ovarian, and small cell lung cancers. However, significant nephrotoxicity has limited its use as 30% of the patients undergoing cisplatin chemotherapy develop dose-dependent AKI.<sup>9,11</sup> Although the molecular mechanisms involved in cisplatin nephrotoxicity are not very well understood, we have shown that the induction of HO-1 in the proximal tubules after cisplatin treatment is protective.<sup>3</sup> Previous work has suggested that increased ROS is one of the cytotoxic mechanisms by which cisplatin causes cell death.<sup>33</sup> In addition, recent evidence indicates that ROS is capable of inducing autophagy.<sup>34,35</sup> Several groups have also shown that autophagy is induced during cisplatin nephrotoxicity and confers protection by delaying apoptosis.<sup>13,22</sup> However, despite its predominant role as a survival mechanism, prolonged autophagy can result in cell death when cells are under persistent stress. Therefore, in this study we chose to address the role of HO-1 in regulating autophagy and protecting cells from cisplatin injury. We observed that HO-1<sup>-/-</sup> mice ex-

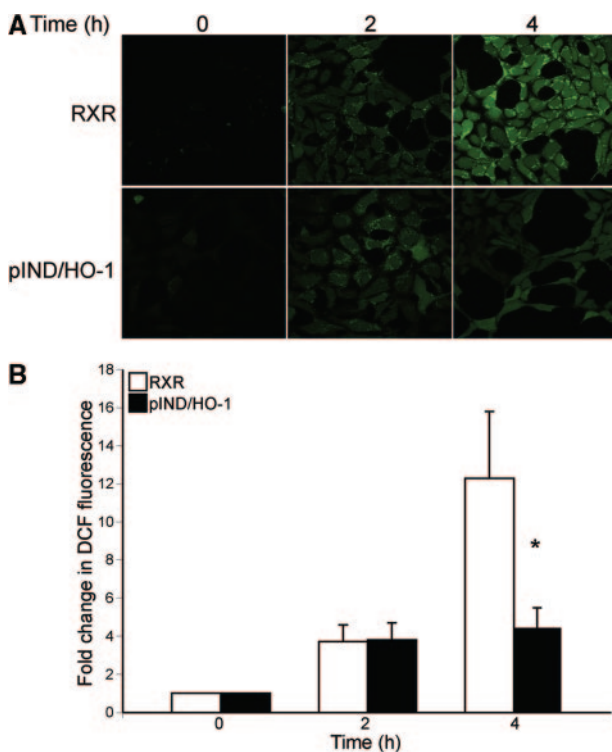


**Figure 9.** Reduced production of reactive oxygen species (ROS) in HO-1 overexpressing (pIND/HO-1) cells after cisplatin treatment. Ecdysone-inducible stable clones were treated with cisplatin (50  $\mu\text{M}$ ) for the indicated times and cells were loaded with 2.5  $\mu\text{M}$  H<sub>2</sub>DCF-DA for 1 hour. (A) Cells were imaged for DCF fluorescence by confocal microscopy. (B) Fluorescence intensity was measured in 8 fields and at least 40 different regions of interest per field and averaged from four independent experiments. Results are expressed as fold increase in DCF fluorescence (ROS) in cisplatin-treated cells compared with untreated cells. \* $P < 0.05$  versus 4-hour-treated RXR group.

hibit a significantly higher number of autophagosomes in the kidney even in saline-treated animals. This supports our finding that HO-1 deficiency leads to elevated basal autophagy and increased apoptosis upon cisplatin injury. Importantly, we also show that overexpression of HO-1 decreases intracellular ROS, delays autophagy, and protects cells from apoptosis after cisplatin injury.

*In vivo*, autophagic vesicles have been visualized by TEM in mice administered cisplatin. As expected, few, if any, vesicles were observed in the wild-type saline-treated kidneys. This is most likely indicative of the constitutive basal autophagy that occurs in cells to maintain homeostasis. Several factors may contribute to the elevated autophagy displayed in the HO-1<sup>-/-</sup> mice, including heme, iron loading, and increased levels of lipid peroxidation and oxidized proteins in the kidneys of these mice.<sup>36</sup> Furthermore, increased oxidative stress and heme levels were also reported in a HO-1-deficient human patient.<sup>37</sup> Although the role of these defects in autophagy induction has not yet been established, it is believed that damaged/oxidized proteins and oxidative stress can result in increased autophagy. Bohensky *et al.* have shown that knock-down of hypoxia-inducible factor 2 resulted in increased intracellular ROS production and oxidative stress, accompanied by an elevated basal autophagy in chondrocytes. In the presence of ROS inhibitors, basal autophagy levels were reduced to that seen in wild-type chondrocytes.<sup>38</sup>

Overexpression of other antioxidants such as manganese-superoxide dismutase and catalase decrease autophagy and protect cells from death in response to oxidative stress.<sup>39,40</sup> In animal models, pretreatment with antioxidants such as vitamin E and  $\gamma$ -glutamylcysteinyl ethyl ester protect against neuronal injury and is accompanied by downregulation of autophagy.<sup>41,42</sup> Overexpression of HO-1 in lung epithelial cells downregulated both ROS generation and autophagy during cigarette smoke extract-induced injury.<sup>43</sup> Similarly, we demonstrate that overexpression of HO-1 in kidney epithelial cells significantly reduced ROS generation compared with that in control cells after cisplatin treatment, while delaying the onset of autophagy induction and conferring protection. This demonstrates that the antioxidant effect of HO-1 partially delays the onset of autophagy without completely inhibiting it. Therefore, we believe that HO-1 protects cells from apoptosis both as an antioxidant and as a modulator of autophagy.

HO-1 may also regulate autophagy via beclin. Our study demonstrates that, in the basal state, beclin is upregulated in the HO-1<sup>-/-</sup> PTC compared with wild-type PTC. Beclin can bind and sequester antiapoptotic proteins, Bcl-2 and Bcl-X<sub>L</sub>, and sensitize cells to apoptosis in an injurious setting.<sup>44–46</sup> This could also be one of the mechanisms by which HO-1<sup>-/-</sup> PTC are susceptible to cisplatin injury. Recent evidence by Kim *et al.* indicates that overexpression of HO-1 can significantly reduce the expression of beclin in lung epithelial cells and inhibit autophagy during cigarette smoke-induced injury.<sup>43</sup> It is therefore likely that HO-1 overexpression may also mediate its antiapoptotic and antiautophagic effects through downregulation of beclin during cisplatin injury.

Studies show that the role of autophagy in cell survival is dependent upon the amount of stress a cell undergoes. Periyasamy-Thandavan *et al.* showed that mild stress induced autophagy alone, but severe stress induced autophagy accompanied by apoptosis.<sup>13</sup> Induction of autophagy during the initial period of cisplatin insult may efficiently eliminate damaged proteins, organelles, and other macromolecules to establish cellular homeostasis before reaching the threshold for cisplatin-induced apoptosis.<sup>22</sup> The absence of HO-1 may create an oxidative environment, which lowers the threshold for injury after cisplatin administration, resulting in heightened apoptosis. The results of this study show that although HO-1<sup>-/-</sup> PTC have elevated basal autophagy, they are unable to respond to cisplatin injury with an additional induction of autophagy. These cells undergo apoptosis more readily than wild-type cells. This illustrates the importance of regulation of autophagy, and not simply its presence or absence in cell survival. Importantly, our findings demonstrate that induction of autophagy, reduced basal autophagy, and decreased cleaved caspase-3 levels can be achieved by restoring HO-1 gene expression. This suggests that HO-1 may also be a key mediator in the balance between autophagy and apoptosis.

In conclusion, we have shown that the absence of HO-1 results in impaired autophagy and increased apoptosis after cisplatin in renal epithelial cells. Restoring HO-1 expression in these cells reversed the impaired autophagic response and decreased susceptibility to cisplatin-induced apoptosis, validating the importance of HO-1 expression during cisplatin injury. Also, overexpression of HO-1 inhibited ROS generation, concurrently delayed the onset of autophagy, and decreased cell death after cisplatin injury. On the basis of the findings of this study, a proposed hypothetical model that depicts the role of HO-1 in cisplatin-induced autophagy and apoptosis is sche-

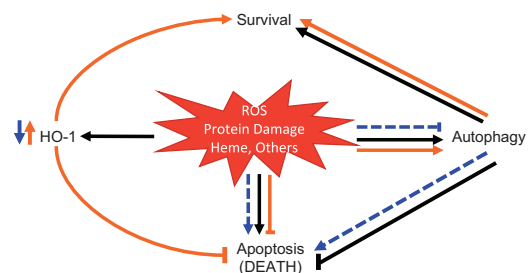


**Figure 10.** Schematic showing the role of HO-1, ROS, and heme in autophagy. During cisplatin injury (black arrows), increased ROS leads to destabilization of heme-containing proteins and increased free heme levels in the cell. Autophagy and HO-1 are induced during this insult to overcome the oxidative stress and serve as adaptive responses to protect from cell death. In the absence of HO-1 (blue arrows), the oxidative environment in the cell is further exaggerated after cisplatin by an increase in levels of free unmetabolized heme (substrate), heightened generation of ROS, and oxidative stress, thereby leading to dysregulated autophagy and cell death. Overexpression of HO-1 (orange arrows) limits heme accumulation, ROS generation, and oxidative stress during cisplatin injury, and hence delays the onset of autophagy and promotes survival.

matized in Figure 10. HO-1 and autophagy are induced after cisplatin to overcome oxidative stress and serve as adaptive responses to prevent cell death. The absence of HO-1 is associated with increased levels of free unmetabolized heme (substrate), heightened generation of ROS, and oxidative stress. The latter is further exaggerated after exposure to cisplatin, leading to dysregulated autophagy and cell death. Additionally, HO-1 overexpression is able to limit heme accumulation, ROS generation, and oxidative stress during cisplatin injury, and thereby significantly inhibiting autophagy and apoptosis. These results highlight the role of HO-1 in limiting oxidative stress and regulating autophagy and determining the fate of cells during cisplatin injury. Targeting HO-1 as a modulator of autophagy may result in novel therapeutic interventions in AKI.

## CONCISE METHODS

### Animals

HO-1<sup>-/-</sup> and HO-1<sup>+/+</sup> mice [8 to 12 weeks of age, (C57BL/6xFVB)F<sub>1</sub>] were used for both *in vitro* and *in vivo* studies. A humanized HO-1 transgenic mouse line (HBAC), expressing only the human HO-1 gene, were generated using a human bacterial artificial chromosome clone (Kim J, Agarwal A, in preparation). Briefly, an 87-Kb bacterial artificial chromosome DNA from chromosome 22 (accession no. z82244) containing the human HO-1 gene was microinjected into oocytes from C57BL/6 mice, which were then implanted into pseudopregnant female mice. After birth, potential founders were screened for the presence of the transgene using PCR with human HO-1 specific primers. Animals positive for the transgene were then mated with HO-1<sup>-/-</sup> mice to generate human HO-1-expressing HBAC mice that were screened using PCR for the presence of the human HO-1 gene and the absence of the mouse HO-1 gene. HBAC mice were characterized for the expression of mouse and human HO-1 mRNA transcripts in the kidney by real-time PCR. HBAC mice (8 to 14 weeks of age) were used to generate primary renal proximal tubular cells.

### Generation of Proximal Tubule Epithelial Cells from Mice

Primary PTC cultures were generated from the kidneys of HBAC, HO-1<sup>-/-</sup>, and their wild-type littermates using a previously described procedure with minor modifications.<sup>47,48</sup> Kidney cortices from mice were dissected from the medulla, sliced, minced, and filtered through a 70- $\mu$ m cell strainer over a 50-ml conical tube with media (Renal Epithelial Cell Growth Medium; PromoCell). The medium containing the tubules was centrifuged and plated on collagen-coated culture plates and then incubated for 72 hours at 37°C in 5% CO<sub>2</sub>. Each experiment required PTC generated from a single animal and cells were not passaged. Cells were examined for expression of  $\gamma$ -glutamyltranspeptidase and alkaline phosphatase, markers for proximal tubule cells, as described previously.<sup>47</sup>

### Cisplatin Injury Model

HO-1<sup>-/-</sup> and HO-1<sup>+/+</sup> mice were administered 20 mg/kg body wt cisplatin (1.0 mg/ml solution in sterile normal saline) or vehicle (nor-

mal saline) by a single intraperitoneal injection. Mice were sacrificed 24 and 72 hours after cisplatin administration. Kidneys were harvested, cut transversely, and fixed in 10% neutral buffered formalin for immunohistochemistry. The animal protocol was approved by the Institutional Animal Care and Use Committee at the University of Alabama at Birmingham. For *in vitro* experiments, 50  $\mu$ M cisplatin was added to PTC or HEK293 cells in culture medium and analyzed at indicated time points by real-time PCR or Western blot analysis.

### Electron Microscopy

Renal tissues were fixed at room temperature with a fixative containing 2.5% glutaraldehyde, 1% formaldehyde, 100 mM sodium phosphate, pH 7.2. Samples were rinsed in 0.1 M Na cacodylate (pH 7.4), then postfixed for 1 hour in 2% osmium tetroxide in 0.1 M Na cacodylate, and washed in 0.1 M Na cacodylate. The samples were dehydrated in a graded series of ethanols and propylene oxide and embedded in epoxy resin (Taab 812 Resin; Marivac Industries, Montreal, CA). Ultrathin (60 to 70 nm) sections were counterstained with uranyl acetate and lead citrate and then observed using an Hitachi 7600 transmission electron microscope (Hitachi High-Technologies America, Schaumburg, IL) equipped with a Macrofire monochrome progressive scan CCD camera (Optronics, Goleta, CA) and AMTv image capture software (Advanced Microscopy Techniques, Danvers, MA).

### Immunofluorescence

Paraffin-embedded kidney sections were cut at 4- $\mu$ m thickness and deparaffinized using CitriSolv. Citrate antigen retrieval was performed followed by incubation in 3% hydrogen peroxide solution to block endogenous peroxidase activity. Sections were incubated for 1 hour at room temperature in blocking buffer (1% BSA, 0.2% nonfat dry milk, and 0.3% Triton X-100 in PBS) and then exposed to primary antibody (Ab), rabbit anti-LC3B (1:5000), overnight at 4°C. Sections were washed and incubated for 1 hour at room temperature with secondary Ab, SuperPicTure goat anti-rabbit (1:20 dilution; Invitrogen, Carlsbad, CA). Ab binding was detected using TSA Plus Cyanine 3 System and visualized by fluorescence microscopy. Quantitation was performed on slides that were blinded to the reviewer using at least 3 to 6 different fields per time point with an average of 25 renal proximal tubules per field from at least 3 to 6 animals per group.

### Real-Time PCR Analysis

RNA was isolated from cells using TRIzol (Invitrogen) according to the manufacturer's protocol. Three micrograms of RNA was used to convert to cDNA using the First Strand cDNA Synthesis Superscript kit (Invitrogen) according to the manufacturer's protocol. Quantitative real-time PCR was performed with SYBR Green Mastermix (Invitrogen) and 15 pmol primers for mouse HO-1, human HO-1, Atg5, Atg7, and GAPDH. Reactions were performed in triplicate and specificity was monitored using melting curve analysis after cycling. Primers used were as follows (5'-3'): mouse HO-1, 5'-GGTGATGGCTTCCTGTACC-3' and 5'-AGTGAGGCCATACCAGAAG-3'; human HO-1, 5'-CATGACACCAAGGACCAGAG-3' and 5'-AGTGTAAAGACCCATCGGAG-3'; Atg5, 5'-GACGTTGGTAACTGACAAAAGTGA AAAAGCA-3' and 5'-CCAAGGAAGAGCTGAACTTGATGCAAG-3'; Atg7, 5'-CAATCT-

GGGCTAAATGCCATTCTGGAAG-3' and 5'-AGCCCAGTACCCTGGATGG-3'; GAPDH, 5'-TCCCCTCTCCACCTTCGA-3' and 5'-AGTTGGGATAGGGCCTCTCTTG-3'. Relative mRNA expression was quantified using the  $\Delta\Delta$  Ct method and GAPDH was used as an internal control. Results were expressed as fold change over untreated cells.

### Western Blot Analysis

Immunoblot analysis was performed as described previously.<sup>47</sup> Briefly, cell cultures were lysed in RIPA buffer, electrophoresed in a 15% SDS-polyacrylamide gel, and transferred onto a Hybond C Extra membrane (Amersham Biosciences). Membranes were incubated with anti-HO-1 (1:5000 dilution; Stressgen), anti-LC3 (1:2000 dilution, Sigma-Aldrich), anti-cleaved caspase-3 (1:2000 dilution; Cell Signaling), anti-beclin (1:2000 dilution; Santa Cruz Biotechnology), or anti-Atg5 (1:5000 dilution; Millipore) antibodies, followed by a peroxidase-conjugated goat anti-rabbit (or mouse) IgG antibody (1:10000 dilution; Jackson ImmunoResearch Laboratories, West Grove, PA). Horseradish peroxidase activity was detected using enhanced chemiluminescence. The membrane was stripped and probed with anti-actin antibody (1:5000 dilution; Sigma-Aldrich) to confirm loading and transfer. Results were normalized to actin or LC3-I and expressed as fold change over untreated cells.

### Plasmids and Generation of Inducible HO-1 Overexpressing HEK293 cells

pVgRXR regulatory vector and pIND-inducible vector (ecdysone-inducible mammalian expression system; Invitrogen) were used to generate inducible HO-1 overexpressing HEK293 cells. The entire protein-coding region of the human HO-1 gene was cloned into the EcoRI and XbaI sites of the pIND vector to generate the pIND/HO-1 inducible vector. Pon A (Invitrogen) was used to induce expression of genes under the regulation of the ecdysone-inducible expression system.

HEK293 cells were transfected with pVgRXR regulatory vector using lipofectamine 2000 (Invitrogen) and stable clones were selected with the addition of zeocin (400  $\mu$ g/ml; Invitrogen). Individual clones were isolated and maintained with 100  $\mu$ g/ml zeocin. Inducible HO-1 overexpressing HEK293 cells were generated by stably transfecting pVgRXR cells with the pIND/HO-1 plasmid and selected with the addition of geneticin (600  $\mu$ g/ml). Individual clones were isolated and maintained with 100  $\mu$ g/ml zeocin and 200  $\mu$ g/ml geneticin. HEK293 cells stably transfected with pVgRXR are referred to as RXR cells and serve as control. HEK293 cells stably transfected with pVgRXR and pIND/HO-1 vector are referred to as pIND/HO-1 cells. Stable cells were maintained in Dulbecco's Minimum Essential Medium supplemented with fetal bovine serum (5%), glutamine, antibiotic-antimycotic (1 $\times$ ), and HEPES (25 mM) at 37°C in 90% air–10% carbon dioxide. To overexpress HO-1, pIND/HO-1 cells were plated to 70% confluency, serum-starved, and induced with 5  $\mu$ M Pon A for 24 hours. RXR cells treated with 5  $\mu$ M Pon A served as controls.

The GFP-LC3 plasmid was a generous gift from Dr. Gur Kaushal (University of Arkansas for Medical Sciences, Little Rock, Arkansas). Transfections were performed with lipofectamine 2000 (Invitrogen) according to the manufacturer's protocol.

### HO Enzyme Activity Measurement

HO activity was measured by bilirubin generation as described previously.<sup>3,49</sup> Briefly, cell lysates were centrifuged at 10,000g and supernatant was incubated with rat liver cytosol (3 mg), a source of biliverdin reductase, hemin (20  $\mu$ M), glucose-6-phosphate (2 mM), glucose-6-phosphate dehydrogenase (0.2  $\mu$ ), and NADPH (0.8 mM) for 1 hour at 37°C in the dark. The bilirubin formed was extracted with chloroform;  $\Delta$ optical density of 464 to 530 nm was measured and enzyme activity was calculated as picomoles of bilirubin formed per 60 minutes per milligram of protein. Fold change in HO activity was determined by comparing the activity of HO-1 overexpressing cells to RXR control cells.

### Cell Viability Assay

Cells were plated in 24-well plates and allowed to reach 70% confluency, serum-starved, and treated with 5  $\mu$ M Pon A for 24 hours. Cells were incubated with 50  $\mu$ M hemin or 100  $\mu$ M cisplatin for 24 hours. Adherent cells were lifted gently by treatment with diluted trypsin and floating cells collected from the media. Cell suspensions were incubated with equal volumes of trypan blue for 5 minutes and observed under a microscope. The viable cells that excluded the dye and dead cells that did not were counted and cell viability was expressed as % live cells/total number of cells.

### Detection of Autophagosomes by GFP-LC3

Primary mouse PTC cultures and HO-1 overexpressing or RXR control HEK293 cells were plated on chamber slides, grown to 60% confluency, and transfected with pGFP-LC3 (0.5  $\mu$ g/ml) using lipofectamine 2000 (Invitrogen) according to manufacturer's protocol. PTC were allowed to reach 80% confluency and treated with 50  $\mu$ M cisplatin for the times indicated. pIND/HO-1 and RXR cells were induced with Pon A for 24 hours, after which they were treated with cisplatin (50  $\mu$ M) for the detection of autophagosomes. Cells were fixed at the end of incubation in cold methanol, mounted, and observed under an inverted fluorescence microscope. Cells with diffuse and punctated GFP-LC3 were counted and autophagosome formation was expressed as % punctated GFP-LC3 expression/total number of cells expressing GFP-LC3. Quantitation was performed in a blinded fashion on at least 12 different fields per time point with an average of 50 cells from at least three independent experiments. Confocal imaging was performed to emphasize the expression pattern of GFP-LC3 after cisplatin treatment.

### Measurement of ROS

ROS generation was measured as described previously.<sup>50</sup> Briefly, RXR and pIND/HO-1 cells were plated on collagen-coated chamber slides, induced with Pon A, and treated with 50  $\mu$ M cisplatin for the times indicated. Cells were loaded with 2.5  $\mu$ M 2',7'-2',7'-dichlorodihydrofluorescein diacetate [ $H_2$ DCF-DA (Invitrogen)] for 1 hour before imaging. Cells were imaged with a laser-scanning confocal scan head (Olympus FV300) mounted on an inverted fluorescence microscope (Olympus IX71) equipped with oil immersion objectives (Olympus 60 $\times$  1.2NA). DCF fluorescence was excited with an Ar laser (488 nm) and its emission filtered at 510  $\pm$  20 nm. Single images were scanned at 512  $\times$  512 pixel resolution (1.96 seconds per frame), avoiding PMT

saturation (400 to 500 V PMT voltage,  $1\times$  gain, zero offset), saved as TIFF files, and analyzed using ImageJ (National Institutes of Health). The average pixel intensity within a single region of interest defined around individual cells in DCF dye fluorescence images was used for quantitative estimation of ROS levels. Fluorescence intensity was measured in 8 fields and at least 40 different regions of interest per field and averaged from four independent experiments. Results are expressed as fold increase in DCF fluorescence (ROS) in cisplatin-treated cells compared with untreated cells.

### Statistical Analysis

Data are presented as mean  $\pm$  SEM. The *t* test was used for comparisons between two groups. For the comparisons that involved more than two groups, ANOVA and the Newman-Keuls test were used for analysis, with statistical significance considered at  $P < 0.05$ .

### ACKNOWLEDGMENTS

We thank Dr. Gur Kaushal (University of Arkansas for Medical Sciences, Little Rock, AK) for generously providing us the GFP-LC3 plasmid. We thank Dr. Jill W. Verlander and George Kasnic for the ultrastructural studies that were conducted at the University of Florida College of Medicine Electron Microscopy Core Facility. We also thank Syreeta M. Davis and Cecelia B. Latham for their help with the immunofluorescence studies that were conducted at the University of Alabama at Birmingham Neuroscience Molecular Detection Core under grant P30 NS0474666.

This work was supported by the National Institutes of Health R01 Grants DK59600, DK75532, and P30 DK079337 O'Brien Core Center for acute kidney injury research to A.A. and American Heart Association pre-doctoral fellowship award 0815026E to S.B.

Part of this material was presented in abstract form at the annual meeting of the American Society of Nephrology; October 27 through November 1, 2009; San Diego, CA.

### DISCLOSURES

None.

### REFERENCES

- Baliga R, Ueda N, Walker PD, Shah SV: Oxidant mechanisms in toxic acute renal failure. *Am J Kidney Dis* 29: 465–477, 1997
- Devarajan P: Update on mechanisms of ischemic acute kidney injury. *J Am Soc Nephrol* 17: 1503–1520, 2006
- Agarwal A, Balla J, Alam J, Croatt AJ, Nath KA: Induction of heme oxygenase in toxic renal injury: A protective role in cisplatin nephrotoxicity in the rat. *Kidney Int* 48: 1298–1307, 1995
- Nath KA: Heme oxygenase-1: A provenance for cytoprotective pathways in the kidney and other tissues. *Kidney Int* 70: 432–443, 2006
- Agarwal A, Nick HS: Renal response to tissue injury: Lessons from heme oxygenase-1 gene ablation and expression. *J Am Soc Nephrol* 11: 965–973, 2000
- Maines MD: The heme oxygenase system: A regulator of second messenger gases. *Annu Rev Pharmacol Toxicol* 37: 517–554, 1997
- Sikorski EM, Hock T, Hill-Kapturczak N, Agarwal A: The story so far: Molecular regulation of the heme oxygenase-1 gene in renal injury. *Am J Physiol Renal Physiol* 286: F425–F441, 2004
- Nath KA, Haggard JJ, Croatt AJ, Grande JP, Poss KD, Alam J: The indispensability of heme oxygenase-1 in protecting against acute heme protein-induced toxicity in vivo. *Am J Pathol* 156: 1527–1535, 2000
- Ries F, Klastersky J: Nephrotoxicity induced by cancer chemotherapy with special emphasis on cisplatin toxicity. *Am J Kidney Dis* 8: 368–379, 1986
- Safirstein R, Winston J, Goldstein M, Moel D, Dikman S, Guttenplan J: Cisplatin nephrotoxicity. *Am J Kidney Dis* 8: 356–367, 1986
- Shiraishi F, Curtis LM, Truong L, Poss K, Visner GA, Madsen K, Nick HS, Agarwal A: Heme oxygenase-1 gene ablation or expression modulates cisplatin-induced renal tubular apoptosis. *Am J Physiol Renal Physiol* 278: F726–F736, 2000
- Kaushal GP, Kaushal V, Herzog C, Yang C: Autophagy delays apoptosis in renal tubular epithelial cells in cisplatin cytotoxicity. *Autophagy* 4: 710–712, 2008
- Periyasamy-Thandavan S, Jiang M, Wei Q, Smith R, Yin XM, Dong Z: Autophagy is cytoprotective during cisplatin injury of renal proximal tubular cells. *Kidney Int* 74: 631–640, 2008
- Matsui Y, Takagi H, Qu X, Abdellatif M, Sakoda H, Asano T, Levine B, Sadoshima J: Distinct roles of autophagy in the heart during ischemia and reperfusion: Roles of AMP-activated protein kinase and Beclin 1 in mediating autophagy. *Circ Res* 100: 914–922, 2007
- Lieberthal W: Macroautophagy: A mechanism for mediating cell death or for promoting cell survival? *Kidney Int* 74: 555–557, 2008
- Levine B, Yuan J: Autophagy in cell death: An innocent convict? *J Clin Invest* 115: 2679–2688, 2005
- Mizushima N: Autophagy: Process and function. *Genes Dev* 21: 2861–2873, 2007
- Nishida K, Yamaguchi O, Otsu K: Crosstalk between autophagy and apoptosis in heart disease. *Circ Res* 103: 343–351, 2008
- Maiuri MC, Zalckvar E, Kimchi A, Kroemer G: Self-eating and self-killing: Crosstalk between autophagy and apoptosis. *Nat Rev Mol Cell Biol* 8: 741–752, 2007
- Mizushima N, Levine B, Cuervo AM, Klionsky DJ: Autophagy fights disease through cellular self-digestion. *Nature* 451: 1069–1075, 2008
- Yorimitsu T, Klionsky DJ: Eating the endoplasmic reticulum: Quality control by autophagy. *Trends Cell Biol* 17: 279–285, 2007
- Yang C, Kaushal V, Shah SV, Kaushal GP: Autophagy is associated with apoptosis in cisplatin injury to renal tubular epithelial cells. *Am J Physiol Renal Physiol* 294: F777–F787, 2008
- Klionsky DJ, Cregg JM, Dunn WA Jr, Emr SD, Sakai Y, Sandoval IV, Sibiry A, Subramani S, Thumm M, Veenhuis M, Ohsumi Y: A unified nomenclature for yeast autophagy-related genes. *Dev Cell* 5: 539–545, 2003
- Xie Z, Klionsky DJ: Autophagosome formation: Core machinery and adaptations. *Nat Cell Biol* 9: 1102–1109, 2007
- Kabeya Y, Mizushima N, Ueno T, Yamamoto A, Kirisako T, Noda T, Kominami E, Ohsumi Y, Yoshimori T: LC3, a mammalian homologue of yeast Apg8p, is localized in autophagosomal membranes after processing. *EMBO J* 19: 5720–5728, 2000
- Cao Y, Klionsky DJ: Physiological functions of Atg6/Beclin 1: A unique autophagy-related protein. *Cell Res* 17: 839–849, 2007
- Dong Z, Wang L, Xu J, Li Y, Zhang Y, Zhang S, Miao J: Promotion of autophagy and inhibition of apoptosis by low concentrations of cadmium in vascular endothelial cells. *Toxicol In Vitro* 23: 105–110, 2009
- Suzuki C, Isaka Y, Takabatake Y, Tanaka H, Koike M, Shibata M, Uchiyama Y, Takahara S, Imai E: Participation of autophagy in renal ischemia/reperfusion injury. *Biochem Biophys Res Commun* 368: 100–106, 2008
- Wu HH, Hsiao TY, Chien CT, Lai MK: Ischemic conditioning by short periods of reperfusion attenuates renal ischemia/reperfusion induced apoptosis and autophagy in the rat. *J Biomed Sci* 16: 19, 2009
- Sadoshima J: The role of autophagy during ischemia/reperfusion. *Autophagy* 4: 402–403, 2008

31. Matsui Y, Kyoj S, Takagi H, Hsu CP, Hariharan N, Ago T, Vatner SF, Sadoshima J: Molecular mechanisms and physiological significance of autophagy during myocardial ischemia and reperfusion. *Autophagy* 4: 409–415, 2008
32. Gozuacik D, Bialik S, Raveh T, Mitou G, Shohat G, Sabanay H, Mizushima N, Yoshimori T, Kimchi A: DAP-kinase is a mediator of endoplasmic reticulum stress-induced caspase activation and autophagic cell death. *Cell Death Differ* 15: 1875–1886, 2008
33. Davis CA, Nick HS, Agarwal A: Manganese superoxide dismutase attenuates Cisplatin-induced renal injury: Importance of superoxide. *J Am Soc Nephrol* 12: 2683–2690, 2001
34. Liu Z, Lenardo MJ: Reactive oxygen species regulate autophagy through redox-sensitive proteases. *Dev Cell* 12: 484–485, 2007
35. Scherz-Shouval R, Shvets E, Fass E, Shorer H, Gil L, Elazar Z: Reactive oxygen species are essential for autophagy and specifically regulate the activity of Atg4. *EMBO J* 26: 1749–1760, 2007
36. Poss KD, Tonegawa S: Heme oxygenase 1 is required for mammalian iron reutilization. *Proc Natl Acad Sci U S A* 94: 10919–10924, 1997
37. Jeney V, Balla J, Yachie A, Varga Z, Vercellotti GM, Eaton JW, Balla G: Pro-oxidant and cytotoxic effects of circulating heme. *Blood* 100: 879–887, 2002
38. Bohensky J, Terkhorn SP, Freeman TA, Adams CS, Garcia JA, Shapiro IM, Srinivas V: Regulation of autophagy in human and murine cartilage: Hypoxia-inducible factor 2 suppresses chondrocyte autophagy. *Arthritis Rheum* 60: 1406–1415, 2009
39. Chen Y, McMillan-Ward E, Kong J, Israels SJ, Gibson SB: Mitochondrial electron-transport-chain inhibitors of complexes I and II induce autophagic cell death mediated by reactive oxygen species. *J Cell Sci* 120: 4155–4166, 2007
40. Yu L, Wan F, Dutta S, Welsh S, Liu Z, Freundt E, Baehrecke EH, Lenardo M: Autophagic programmed cell death by selective catalase degradation. *Proc Natl Acad Sci U S A* 103: 4952–4957, 2006
41. Lai Y, Hickey RW, Chen Y, Bayir H, Sullivan ML, Chu CT, Kochanek PM, Dixon CE, Jenkins LW, Graham SH, Watkins SC, Clark RS: Autophagy is increased after traumatic brain injury in mice and is partially inhibited by the antioxidant gamma-glutamylcysteinyl ethyl ester. *J Cereb Blood Flow Metab* 28: 540–550, 2008
42. Cao L, Xu J, Lin Y, Zhao X, Liu X, Chi Z: Autophagy is upregulated in rats with status epilepticus and partly inhibited by Vitamin E. *Biochem Biophys Res Commun* 379: 949–953, 2009
43. Kim HP, Wang X, Chen ZH, Lee SJ, Huang MH, Wang Y, Ryter SW, Choi AM: Autophagic proteins regulate cigarette smoke-induced apoptosis: Protective role of heme oxygenase-1. *Autophagy* 4: 887–895, 2008
44. Furuya D, Tsuji N, Yagihashi A, Watanabe N: Beclin 1 augmented cis-diamminedichloroplatinum induced apoptosis via enhancing caspase-9 activity. *Exp Cell Res* 307: 26–40, 2005
45. Zhang H, Bosch-Marce M, Shimoda LA, Tan YS, Baek JH, Wesley JB, Gonzalez FJ, Semenza GL: Mitochondrial autophagy is an HIF-1-dependent adaptive metabolic response to hypoxia. *J Biol Chem* 283: 10892–10903, 2008
46. Chien CT, Shyue SK, Lai MK: Bcl-xL augmentation potentially reduces ischemia/reperfusion induced proximal and distal tubular apoptosis and autophagy. *Transplantation* 84: 1183–1190, 2007
47. Kie JH, Kapturczak MH, Traylor A, Agarwal A, Hill-Kapturczak N: Heme oxygenase-1 deficiency promotes epithelial-mesenchymal transition and renal fibrosis. *J Am Soc Nephrol* 19: 1681–1691, 2008
48. Taub M, Sato G: Growth of functional primary cultures of kidney epithelial cells in defined medium. *J Cell Physiol* 105: 369–378, 1980
49. Balla G, Jacob H, Balla J, Rosenberg M, Nath K, Apple F, Eaton J, Vercellotti G: Ferritin: A cytoprotective antioxidant strategem of endothelium. *J Biol Chem* 267: 18148–18153, 1992
50. Ricart KC, Bolisetty S, Johnson MS, Perez J, Agarwal A, Murphy MP, Landar A: The permissive role of mitochondria in the induction of haem oxygenase-1 in endothelial cells. *Biochem J* 419: 427–436, 2009

---

See related editorial, "HO-1 in Control of a Self-Eating Kidney," on pages 1600–1602.